scientific reports



OPEN

Towards a quality control framework for cerebral cortical organoids

Héloïse Castiglione^{1,2,3∞}, Lucie Madrange^{1,2}, Camille Baquerre³, Benoît Guy Christian Maisonneuve^{1,3}, Thomas Lemonnier^{1,2}, Jean-Philippe Deslys², Frank Yates^{1,2}, Thibault Honegger³, Jessica Rontard^{3,4} & Pierre-Antoine Vigneron^{1,2,4∞}

Cerebral organoids offer significant potential for neuroscience research as complex in vitro models that mimic human brain development. However, challenges related to their quality and reproducibility hinder their reliability. Discrepancies in morphology, size, cellular composition, and cytoarchitectural organization limit their applications, particularly in disease modeling, drug screening, and neurotoxicity testing. Critically, current methods for organoid characterization often lack standardization, restricting their broader applicability. To address the need for standardized quality assessment of cerebral organoids, we developed a Quality Control (QC) methodology for 60-day cortical organoids, evaluating five key criteria using a scoring system: morphology, size and growth profile, cellular composition, cytoarchitectural organization, and cytotoxicity. We implemented a hierarchical approach, beginning with non-invasive assessments to exclude low-quality organoids, while reserving in-depth analyses for those that passed the initial evaluation. To validate this framework, we exposed 60-day cortical organoids to graded doses of hydrogen peroxide (H₂O₂), inducing a range of quality outcomes. The QC system demonstrated its robustness by accurately discriminating organoid qualities. Our proposed QC framework is designed to be user-friendly, flexible, and broadly applicable, making it suitable for routine assessment of cerebral organoid quality. Additionally, its scalability enables industrial applications, offering a valuable tool for advancing both fundamental and pre-clinical research.

Keywords Cerebral organoids, Quality control, Hierarchical scoring methodology, Reproducibility, Standardization.

Cerebral organoids have emerged as innovative tools in neuroscience by providing biologically relevant in vitro models that recapitulate aspects of the human brain development and function. These three-dimensional (3D) structures, derived from the neuroectodermal differentiation of pluripotent stem cells, self-organize into complex architectures recapitulating certain regions of the human brain¹, such as the forebrain, midbrain, hindbrain, or even more specifically the hippocampus, cortex, or choroid plexus^{2–12}. Non-specific differentiation protocols can also give rise to unguided whole-brain organoids¹³.

Unlike traditional 2D cultures or simpler 3D models such as spheroids and neurospheres, cerebral organoids recreate a physiologically relevant cellular microenvironment. This complexity enhances cell-cell and cell-matrix interactions, fostering improved differentiation and maturation¹⁴. While human brain organogenesis remains a highly complex process, tightly regulated both on a spatial and a temporal scale¹⁵, cerebral organoids have proven their ability to model key neurodevelopmental aspects, including neurogenesis, neuronal migration, neuromorphogenesis, and synaptogenesis^{1,15}. Furthermore, transcriptomic and epigenetic analyses have revealed that these models closely mimic developmental trajectories observed in the human fetal brain^{15,16}. When derived from patient-specific cells, or when combined with advanced genetic engineering techniques, such features have made cerebral organoids powerful tools for studying neurodevelopmental disorders, such as microcephaly¹³ and trisomy 21^{17–19}, as well as for studying neurological cancers²⁰, and can also give clues about

¹SupBiotech, Ecole d'Ingénieurs en Biotechnologies, Villejuif, France. ²Commissariat à l'Energie Atomique et aux Energies Alternatives (CEA), Service d'Etude des Prions et des Infections Atypiques (SEPIA), Université Paris-Saclay, Fontenay-aux-Roses, France. ³NETRI, Lyon, France. ⁴Jessica Rontard and Pierre-Antoine Vigneron contributed equally to this work. [⊠]email: heloise.castiglione@netri.com; pierre-antoine.vigneron@supbiotech.fr

the pathogenesis of neurodegenerative diseases, including Alzheimer's disease^{21,22}, Parkinson's disease²³, and Creutzfeldt-Jakob disease²⁴.

Beyond modeling diseases, cerebral organoids have shown promise in neurotoxicity studies^{25–27}. Notably, the developing human brain is highly susceptible to environmental insults, and exposure to pollutants or chemicals during pregnancy can disrupt its physiological development. Organoids could provide an unprecedented human-based predictive model to study developmental neurotoxicity (DNT) in response to drugs, chemicals, and pollutants. Studies using cerebral organoids have already explored the effects of valproic acid^{28–35}, nicotine³⁶, cannabis³⁷, bisphenol S^{38,39}, cadmium⁴⁰, and nanoplastics⁴¹, among others^{42–45}.

Despite their potential, cerebral organoids face significant challenges regarding quality and reproducibility. Morphological inconsistencies, variations in size, differences in cellular composition or cytoarchitectural organization, and discrepancies in functional activities often arise from the stochastic nature of stem cell differentiation and the spontaneous self-organization occurring within the organoids 1,46. For instance, within a batch of cerebral organoids, some organoids will display optimal morphology, with dense overall structure and well-defined borders, while others may be poorly compact and will tend to degrade over time by losing cells^{47,48}. Moreover, some organoids will exhibit expected cell types and cytoarchitectural organization, whereas others may present disorganized structures and lower proportions of some cell types. Similarly, suboptimal cystic cavities can also be present within some organoids or protrude from their surface⁴⁷. In addition, a necrotic core can also arise in certain organoids^{1,46,49}. Non-cerebral structures might also occasionally occur, including germ layers other than neuroectoderm, especially in the unguided organoids 1,50. These inconsistencies compromise the reproducibility of scientific results, particularly in disease modeling, neurotoxicity testing, and preclinical drug screening, where high-quality and consistent models are essential⁴⁶. Furthermore, this variability is exacerbated by the lack of standardized criteria for organoid generation, culture, and characterization, and the widespread use of in-lab adaptations, leading to varying quality standards between research groups and creating barriers to their broader adoption in industrial and preclinical applications.

Current methods for organoid characterization, including immunohistochemistry^{2,13}, transcriptomic profiling⁶, electrophysiological recording⁵¹, and cytotoxicity studies^{52–56} are valuable but often lack standardization and face several limitations. Many current approaches rely on qualitative and subjective assessments that might introduce inconsistencies and bias. It is common that for daily evaluation of cerebral organoids, researchers rely on morphological observations to assess quality, but this qualitative readout is not frequently detailed in research publications. Although morphological criteria are often used and provide valuable information, their translation into standardized quantitative indicators transferable between laboratories remains partially done, even if recent publications highlight a growing interest in leveraging these criteria as reliable, non-invasive readouts for characterizing cerebral organoids^{57–59}. Moreover, some analysis methods commonly used in 2D cell cultures are difficult to transpose to 3D cultures, further complicating the standardization of their characterization^{56,60}. Overall, there is a notable lack of robust and well-defined quantitative methodologies for 3D organoid characterization. This gap limits the ability to objectively evaluate cerebral organoids in terms of quality, especially across diverse research groups, ultimately affecting the reliability and consistency of results.

Additionally, this challenge is amplified by the diversity of cerebral organoid types, which depend on the differentiation protocols such as regionalized or unguided whole-brain organoids¹, and the variety of studies, including disease modeling and neurotoxicological evaluation, each requiring different quality standards and pathophysiological phenotypes. Similarly, the long-term cultures of cerebral organoids, ranging from several months to years, also imply different maturation stages associated with specific characteristics, markers and quality criteria^{1,15,61}.

In this study, we propose a Quality Control (QC) framework for 60-day cortical organoids to address these challenges in their evaluation. This system integrates five critical criteria: (A) Morphology, (B) Size and Growth Profile, (C) Cellular Composition, (D) Cytoarchitectural Organization, and (E) Cytotoxicity, into a standardized scoring methodology. The framework is designed hierarchically, prioritizing early, non-invasive evaluations to efficiently exclude organoids of low quality, while reserving in-depth analyses for organoids that have met initial thresholds. To validate its reliability and applicability, we exposed 60-day cortical organoids to gradual doses of hydrogen peroxide (H_2O_2), known to cause oxidative stress-induced cell death at non-physiological doses 62,63, thus producing varying quality levels to rigorously test the scoring system.

The QC methodology we are proposing has been specifically adapted to cortical organoids cultured in vitro for 60 days. For cortical differentiation, 60 days is a critical intermediate stage between so-called immature and mature cortical organoids, characterized by the presence of neural progenitors, as well as neurons and astrocytes⁶¹. This stage also frequently coincides with the presence of rosette structures that model the development of the neural tube^{15,61}, providing key information for studies on neurodevelopmental processes and toxicity in particular.

By minimizing observer bias and enabling objective, reproducible quality assessments, this QC framework enhances the consistency and comparability of results in cerebral organoid research. Moreover, its potential to support both academic studies and industrial scalability highlights its value as a versatile tool for advancing biomedical research.

Results

Quality control enables classification of 60-day cortical organoids by quality level

We developed a comprehensive QC framework based on a scoring methodology adapted to 60-day cortical organoid evaluation and classification (Fig. 1). This QC scoring system is structured around five primary criteria (A to E) corresponding to cortical organoid analysis readouts – (A) Morphology, (B) Size and growth profile, (C) Cellular composition, (D) Cytoarchitectural organization, and (E) Cytotoxicity level – each further subdivided into specific indices (Fig. 1). For each index, cortical organoids are evaluated on a scale of scores between 0 (low

quality) and 5 (high quality). To streamline the process, the criteria are hierarchically organized, prioritizing non-invasive and critical assessments (Fig. 1A). Thresholds with minimum scores are defined for each criterion (Fig. 1B), and failure to meet these thresholds halts further QC evaluation, categorizing the organoid as low-quality and resulting in its exclusion from the study. In cases where all minimal scores are achieved for a criterion, additional composite thresholds, integrating multiple indices, are applied to ensure a robust quality classification (Fig. 1B). For a detailed, illustrated and easy-to-use version of the QC scoring, see Fig. S1 in the Supplementary Information.

This scoring system is designed for two applications: (1) an Initial QC, which relies exclusively on the first two non-invasive criteria (A and B) to determine eligibility of the organoids before entering a study (pre-study QC), and (2) a Final QC based on all the scoring criteria for a complete analysis at the end of a study (post-study QC) (Fig. 1A). Minimal thresholds have also been determined for passing the Initial and Final QC (Fig. 1B).

To validate this QC scoring methodology, we subjected cortical organoids at 60 days of culture to increasing doses of hydrogen peroxide (H_2O_2) , a chemical known to cause oxidative stress-induced cellular death 62,63 , to generate organoids with varying quality levels (Fig. 1C). In this context, organoids were first selected for the H_2O_2 treatment experiment within a batch of cortical organoids, using the Initial QC method. H_2O_2 exposures were followed by a recovery period of one week, after which the exposed and non-exposed cortical organoids were evaluated for post-treatment quality using the complete Final QC.

Initial quality control scoring streamlines the selection of cortical organoids based on non-invasive criteria

By day 60 of culture, organoids exhibited spontaneous variability in quality due to the intrinsic heterogeneity and stochasticity of differentiation within organoids. Consequently, we evaluated cortical organoids through the Initial QC based on morphology and size evolutions, to select those eligible for the H_2O_2 exposure experiment (Fig. 2). Regarding the morphology evaluation (criterion A), the first index, A1, referring to organoid density and compactness, consistently achieved maximum scores of 5/5 across all the organoids (Fig. 2A, D). On the contrary, discrepancies were observed between the organoids for the second index A2 related to border integrity, with organoid #47 achieving the highest score of 5/5 (Fig. 2Ae, Fig. 2D), organoids #7 and #44 obtaining a score of 4/5 due to the presence of an area with less-defined border (Fig. 2Aa, d, Fig. 2D), and organoid #29 reaching a low score of 2/5 because of poorly-defined borders, but sufficient to pass the QC index (Fig. 2Ab, Fig. 2D). However, organoid #31 failed to reach the minimum required score for border integrity (Fig. 2Ac, Fig. 2D), and was excluded from further analysis. Additionally, no cyst formation was observed, allowing all organoids to pass this third index A3 (Fig. 1A, D).

Regarding the organoid sizes and growth evolutions (criterion B), organoids #29 and #44 were excluded due to insufficient growth both at day 60 and throughout the culture period (Fig. 2B, C, D). Interestingly, organoid #31 would have failed this QC step as well but it had already been excluded based on the first criterion, emphasizing the relevance of this hierarchical order for QC evaluations. Consequently, only organoids #7 and #47 satisfied the minimum thresholds for the two non-invasive criteria and successfully passed the Initial QC (Fig. 2D). Overall, out of 58 cortical organoids generated within this batch, 10 were excluded due to a score lower than 16/25, representing 17% of the total population.

Final quality control scoring effectively evaluates cortical organoids with varying quality levels

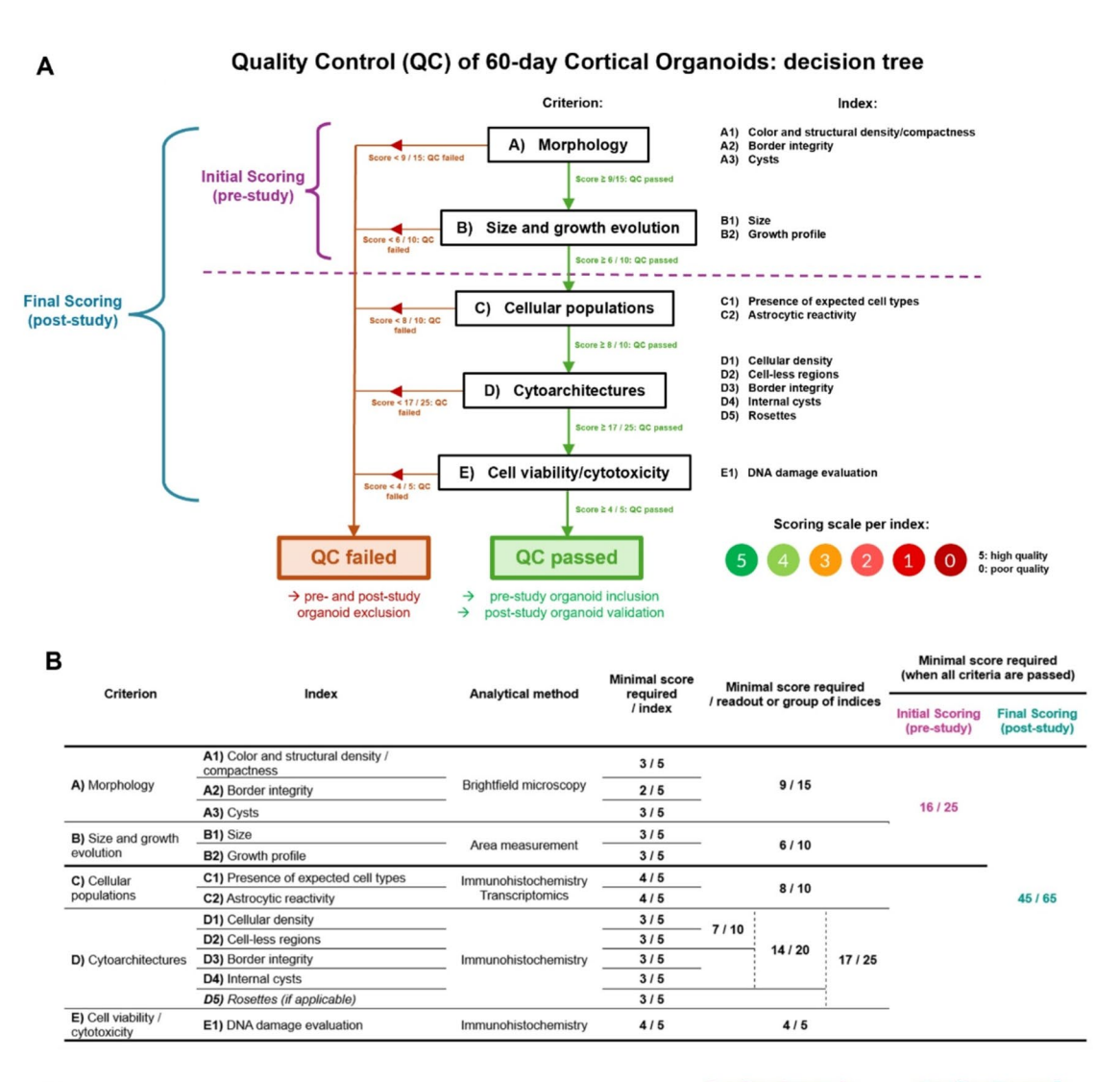
Pre-selected cortical organoids via the Initial QC were included in the H_2O_2 exposure experiment to generate varying degrees of damage (Fig. 3, Fig. S2, Fig. S3). A total of six H_2O_2 concentrations were assayed (n=4 organoids per group): 0% (untreated controls), 0.1%, 0.25%, 0.5%, 1%, and 5% H_2O_2 . Before H_2O_2 exposures, all the organoids exhibited an optimal morphology, resulting from the Initial QC selection (Fig. 3a1-f1, Fig. S2a1-i1, Fig. S3a1-i1). After exposures, organoids exposed to 5% of H_2O_2 displayed severe loss of integrity and cellular disaggregation (Fig. 3f2, Fig. S3g2-i2), thus failing to pass the QC at the morphological criterion for the border integrity index (Table 1, Table S1, Fig. 4). This condition also prevented subsequent analyses based on organoid embedding and sectioning for immunostaining, therefore hampering further QC evaluation for these 5% H_2O_2 -exposed organoids. Organoids treated with the other H_2O_2 concentrations succeeded in passing the morphology QC according to our criteria (Table 1, Table S1).

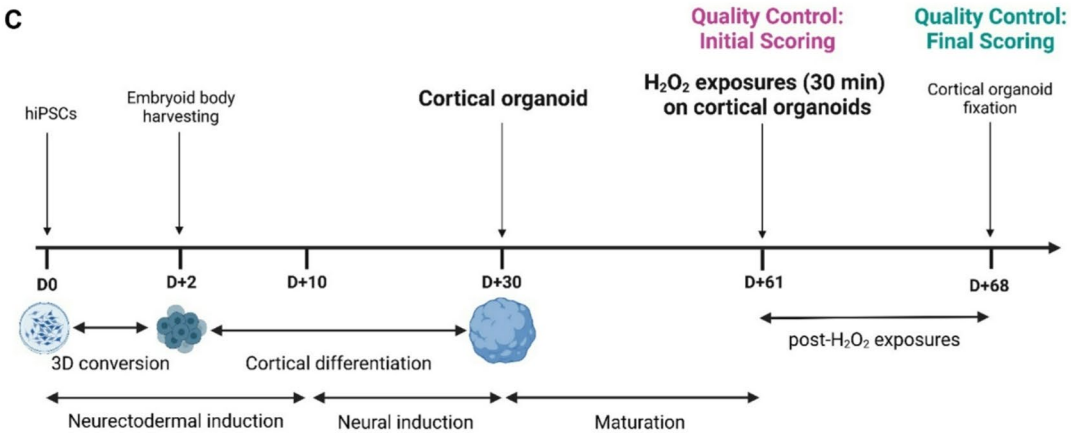
The size and growth profile criterion were not reassessed post- H_2O_2 exposures (Table 1, Table S1), as the seven-day recovery period after H_2O_2 treatment was insufficient for meaningful growth analysis.

Subsequent invasive analyses were performed to evaluate cellular composition and cytoarchitectural organization within the organoids (Fig. 3, Fig. S2, Fig. S3). Immunofluorescence staining confirmed the presence of neural progenitors (SOX2), immature neurons (TUBB3), and astrocytes (GFAP) across all remaining conditions (Fig. 3a3-e6, Fig. S2a3-i6, Fig. S3a3-d6), thus validating the QC criterion of cell type presence verification (Table 1, Table S1). However, it must be noted that three organoids (#23, #30 and #47) could not be analyzed by immunolabeling, as they could not be embedded and sectioned with cryostat, likely due to a lack of compactness. Consequently, these organoids were excluded at this QC step (Table S1). Interestingly, they belonged to conditions where all the other organoids failed to pass the QC indices related to cellular composition and cytoarchitectural assessment (Table 1, Table S1).

Regarding the astrocytic reactivity index, GFAP staining in the remaining organoids treated with $1\%~H_2O_2$ (#51 and #53) suggested a high astrocytic reactivity, by covering 31% and 22% of the section area, respectively (Fig. 3e6, Fig. S3d6). This implies potential physiological disruption, thus excluding these organoids according to our QC criteria.

The next index evaluates the overall cellular density, based on DAPI staining analysis. Among the remaining organoids that have passed previous QC steps, it can be observed that the cellular density was notably reduced





in organoids exposed with 0.5% $\rm H_2O_2$ (#49 and #52), with densities of 6,900 and 7,600 cells.mm $^{-2}$, respectively (Fig. 3d3, Fig. S3b3), therefore not reaching the minimal threshold fixed in the scoring (Fig. S1, Fig. 1B) and leading to the exclusion of these organoids.

In contrast, no significant cytoarchitectural disruptions – such as the presence of large cell-less regions, severely altered borders, or occurrence of internal cysts – were observed in the remaining organoids, which therefore met the minimal QC standards for these criteria (Table 1, Table S1). The rosette index was not assessed in this batch, as neurogenic niches were absent in the control organoids (Table 1, Table S1).

Finally, cytotoxicity was evaluated via γ H2AX staining, a marker of DNA double-stranded breaks, to quantify DNA damage. For all the remaining organoids exposed to 0%, 0.1% and 0.25% $\rm H_2O_2$, the γ H2AX quantification was significantly different from a positive control of maximal γ H2AX labeling (Fig. 3a7-c7, Fig. S2a7-i7), therefore passing this final QC step (Table 1, Table S1). Interestingly, all the organoids exposed to higher doses

∢Fig. 1. Overview of Quality Control methodology for 60-day cortical organoids, and validation by scoring of H₂O₂-exposed cortical organoids. (A) Overview of the Quality Control (QC) adapted to 60-day cortical organoids. The QC relies on several criteria, subdivided into indices, for cortical organoid analysis, including Morphology, Size and growth profile, Presence of expected cellular populations at 60 days, Cytoarchitectural organization, and Cellular viability and cytotoxicity levels. For each index, a scoring system enables the evaluation of organoids based on the attribution of scores ranging from 0 (poor quality) to 5 (high quality). The QC follows a hierarchical structure: criteria are assessed sequentially, and failure to meet an initial criterion automatically classifies the organoid as low quality and subsequent criteria are not assessed. The scoring system is divided into two QC: (1) an Initial Scoring to select cortical organoids before entering a study, based on the first two non-invasive criteria Morphology and Growth; and (2) a Final Scoring for complete analysis of cortical organoids based on all the criteria at the end of a study. (B) Summary table of QC criteria and minimal scores required per index, and per composite groups of indices and readouts, that have to be obtained for cortical organoids to pass the QC. (C) Timeline of cortical organoid generation and culture protocols, including an overview of H₂O₂ exposure conditions. Created with BioRender.com (accessed in November 2024). Before H₂O₂ exposure at D+61, cortical organoids were selected based on the Initial Scoring for QC. Exposed cortical organoids at D+68 were then evaluated following the Final Scoring for complete QC.

than 0.5% H₂O₂, that have been previously excluded at different QC steps, would have failed to pass this final criterion (Fig. 3d7, e7, Fig. S3a7-d7), confirming the validity and relevance of this hierarchical QC system.

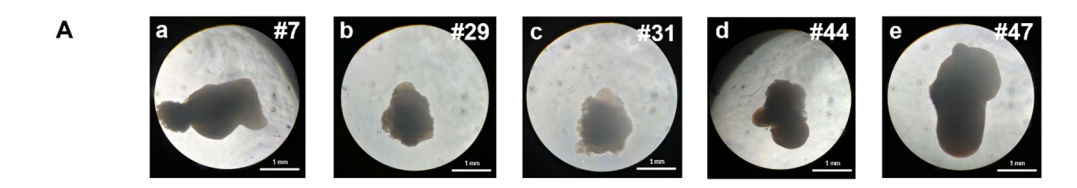
Overall, Fig. 4 summarizes the individual final QC scoring results obtained by all the controls and exposed organoids, as well as the median scores reached per condition. We can observe that the unexposed controls and organoids exposed to the doses of $\rm H_2O_2$ at 0.1% and 0.25% successfully passed the QC. However, organoids treated with doses of 0.5%, 1% and 5% $\rm H_2O_2$ failed to pass the QC evaluation. We can notice that these excluded organoids failed at different QC steps, following the hierarchical order of criteria, with 5% $\rm H_2O_2$ -exposed organoids excluded during the morphological criterion, 1% $\rm H_2O_2$ -exposed organoids failing regarding the cellular composition criterion, and 0.5% $\rm H_2O_2$ -exposed organoids rejected through either the cytoarchitectural or the cytotoxicity criteria (Fig. 4B). Similarly, median scores obtained per condition increase incrementally depending on the exposure doses, from a low score of 5/50 obtained for the highest dose of $\rm H_2O_2$, up to an elevated score of 47/50 reached for the unexposed controls (Fig. 4B), thus correlating with the expected damage levels induced by the $\rm H_2O_2$ graded exposures. These results demonstrate the sensitivity of this QC scoring methodology in efficiently and robustly distinguishing organoid quality levels.

Discussion

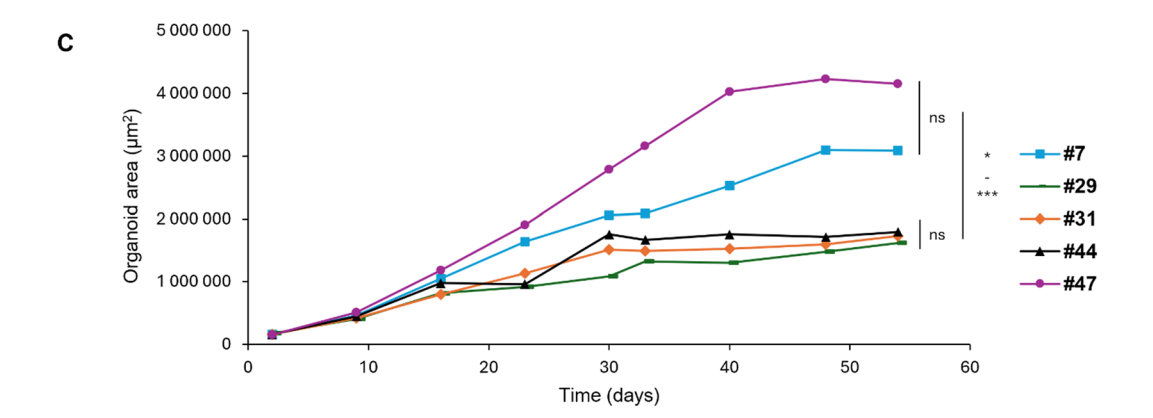
The stochastic nature of the differentiation of stem cells and their spontaneous self-organization within cerebral organoids leads to unpredictable variability among them¹. Consequently, novel approaches have recently emerged to improve culture conditions and enhance organoid reproducibility. Notably, Brain Organoid-on-Chip systems, which rely on the use of microfluidic devices, offer precise fluid flow control and a more physiologically relevant microenvironment⁴⁶, improving cellular viability^{36,37,64,65}, neural maturation^{64,66}, and organoid homogeneity⁶⁴. In addition, the integration of sensors into microfluidic devices further improves real-time organoid monitoring^{27,67}. Flow-based culture systems, including spinning and vertical bioreactors that provide dynamic conditions, enhance differentiation and maturation, by enabling the implementation of mechanochemical, mechanosensing and geometrical transduction effects and better oxygenation in large 3D cultures^{68–72}. Additionally, bioengineering strategies like 3D scaffolds and bioprinting further support structural consistency^{71,73–76}. Advances also focus on increasing cellular complexity through vascularization^{77,78}, incorporation of microglia^{79–82}, co-culture systems⁸³, and assembloids combining region-specific organoids⁸⁴.

A critical gap remains despite these innovations: the absence of consensus on what defines high-quality cerebral organoids. This lack of standardized metrics or guidelines not only hinders meaningful comparisons across studies but also limits the broader applicability of these models. While complete uniformity should not be the goal, since no living systems are identical, excessive variability in cerebral organoid quality undermines their predictability and reproducibility, potentially leading to inaccurate or unreproducible findings, as well as wasted resources. This challenge is further exacerbated by the absence of standardized protocols for organoid generation, culture and characterization, with numerous in-lab adaptations. This pressing need for the establishment of standardized frameworks in the field has been highlighted in recent publications, which urge reaching a consensus on cerebral organoid nomenclature⁸⁵, and describe an experimental framework for designing, conducting and reporting studies with neural organoids, assembloids and their xeno-transplantations⁸⁶. Altogether, this underscores the necessity for user-friendly and broadly applicable quality control methodologies to ensure cerebral organoid reliability in both academic and industrial applications.

Our scoring-based QC approach, adapted to 60-day cortical organoids, opens the way for a standardized quality control methodology (Fig. S1). By incorporating multiple analysis criteria, including both qualitative macro- and micro-level observations, this framework provides a complete evaluation to lay the foundation for defining what constitutes a high-quality cortical organoid. Importantly, our proposed QC is structured hierarchically to rapidly exclude low-quality organoids, while reserving more detailed analyses for those that passed the initial parameters. This scoring system enables precise evaluation of each index and criterion using tailored examples and scoring scales, covering the full quality spectrum observed in cerebral organoids. While morphological criteria remain qualitative, the clarity and preciseness of the provided examples ensure robust evaluations. These illustrative examples enhance accessibility, allowing both experts and non-specialists to apply the scoring method effectively. For the other criteria, quantitative thresholds have been defined. Minimum scores



В				Or	ganoid numb	per	
			#7	#29	#31	#44	#47
	size:	Day 10	465 499	408 551	397 689	451 789	514 644
	Organoid size: area (µm²)	Day 30	2 061 307	1 088 069	1 419 349	1 755 713	2 789 299
	Orga ar	Day 60	3 088 813	1 615 435	1 733 997	1 796 685	4 153 616
		ar regression's pe (area/day)	60 327	26 986	30 503	32 953	88 615



D Recapitulative table of Initial QC A) Morphology B) Size and growth Total score ОC A2) Border A1) Density A3) Cysts B1) Size B2) Growth Initial integrity Scoring result Minima 3/5 2/5 3/5 3/5 3/5 16 / 25 score #7 5 4 5 4 4 22 **Passed** 1 → QC failed Organoid number 5 #29 5 2 13 Failed х 5 #31 6 Failed Х Х х → QC failed 5 5 #44 4 Х 15 Failed → QC failed 5 5 5 5 4 24 Passed #47

Fig. 2. Quality Control (QC) for a selection of cortical organoids before the H_2O_2 exposure experiment, following the Initial Scoring based on the first two non-invasive criteria Morphology and Growth profile. (**A**) Morphology of cortical organoids within a batch at 60 days of culture (brightfield, 5X). (**B**) Table summarizing organoid sizes as surface areas at three timepoints of interest (Day 10, Day 30, and Day 60), as well as slopes of corresponding linear regressions. (**C**) Growth curves of individual organoids from D + 2 to D + 60 of culture. Organoids #29, #31, and #44 display an impaired growth profile significantly different from organoids #7 and #47. Friedman test; n = 4; $p_{31 \text{ vs. } 47} = 0.0175$; $p_{29 \text{ vs. } 27} = 0.0287$; $p_{44 \text{ vs. } 7} = 0.0006$. (**D**) Recapitulative table of scores obtained by the organoids for each readout and index of the Initial QC. Minimal scores per index and the total minimal score required for Initial QC validation are mentioned. Results of QC for each organoid are indicated as Passed/Failed.

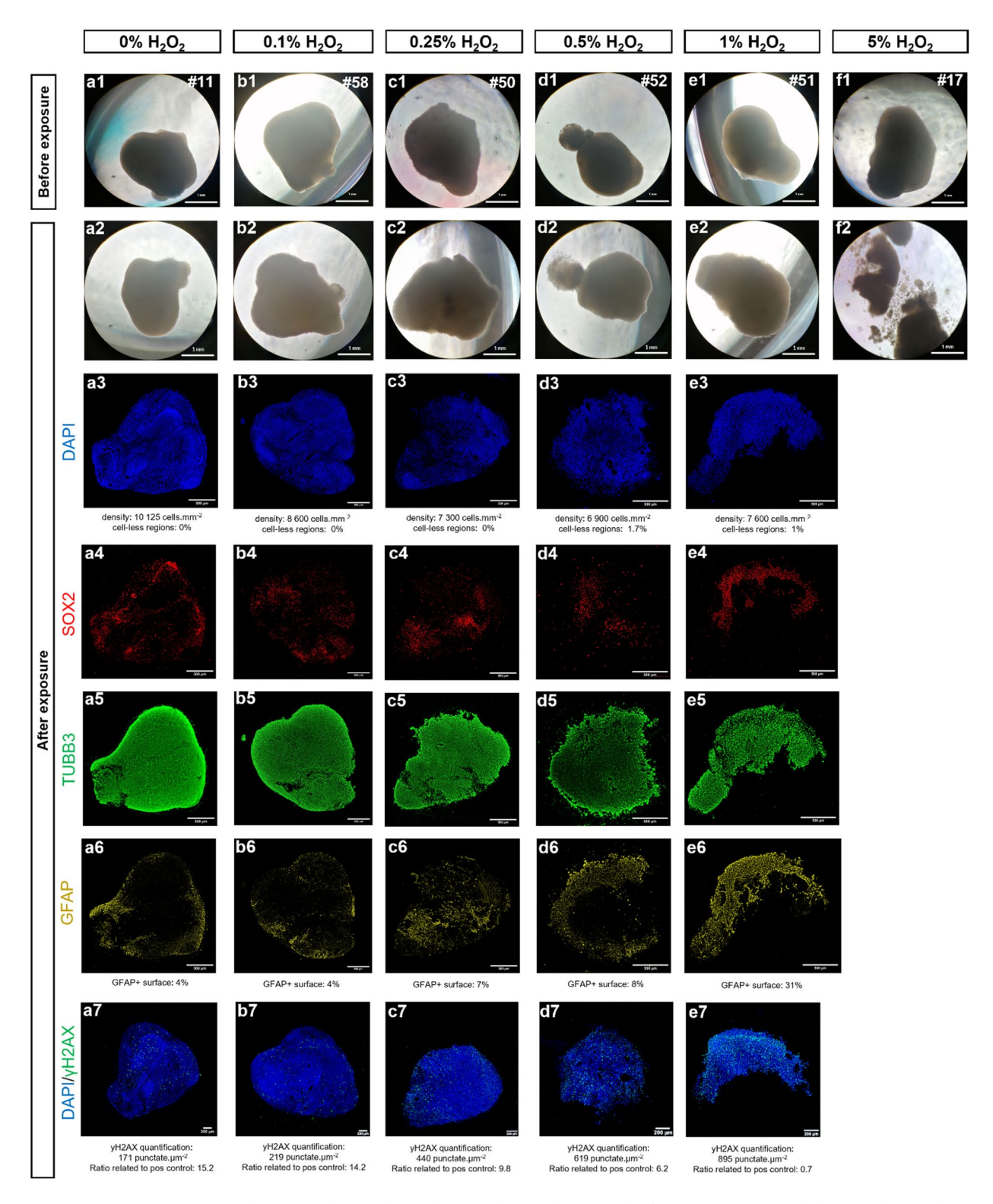
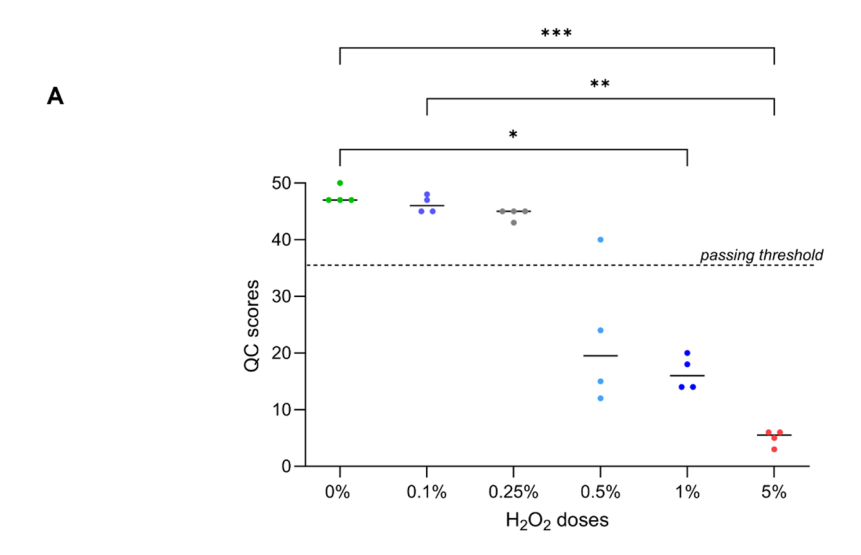


Fig. 3. Quality Control (QC) for evaluation of cortical organoids after H_2O_2 exposures, following the Final Scoring based on all the criteria. H_2O_2 exposures on cortical organoids serve as examples of varying organoid quality levels through incremental H_2O_2 doses. (a1-f1) Examples of cortical organoids exposed to different H_2O_2 doses ranging from 0% to 5%. Morphology before (a1-f1) and after (a2-f2) H_2O_2 exposures serve to evaluate the first criterion related to morphological quality evaluation (brightfield, 5X). Immunofluorescent staining for DAPI (a3-e3), neural progenitor marker SOX2 (a4-e4), neuronal marker TUBB3 (a5-e5), and astrocytic marker GFAP (a6-e6) enable the assessment of the following criteria: verification of cell types presence, assessment of astrocytic reactivity, and evaluation of cytoarchitectural organization. Immunofluorescent labeling of DNA damage with γH2AX marker enables evaluation of cytotoxicity level (a7-e7) (Leica THUNDER microscope, 20X).

	A) Mount of over		B) Size and	and		lotion o	To Complete Strate Company	Contract				E) Cellular viability		
			growm		C) Centinar po	pulations	D) Cytoarciiii	ectural orga	IIIzanon			/ Cytotoxicity		00
v2) Bo ntegr	A2) Border A3) integrity Cys	ts	B1) B2) Size Gro	wth	rpec-	C2) Astrocy-tic reactivity	D1) Cellular Cell-less Border density regions integrity	D2) D3) D4) Cell-less Border Intern regions integrity cysts	D3) Border integrity	D4) Internal D5) cysts Rose	D5) Rosette	E1) DNA damage	Total score	Final Scoring result
H O Organoid Minimal score														
2/5		3/5	3/5 3/5	3/5	4/5	4/5	3/5	3/5	3/5	3/5	3/5	4/5	35/50	
5		5			5	5	5	5	5	5		5	50	Passed
5		4			5	5	3	5	5	5		5	47	Passed
5		5			5	5	3	5	3	5		4	45	Passed
		5	NA		5	5	0 ◊ QC failed	x	x	x	NA	х	24	Failed
3		5			5	0 ◊ QC failed	x	x	×	×		X	18	Failed
QC.	0 ◊ QC failed x	×			×	x	x	×	×	×		X	3	Failed

Table 1. Recapitulative table of H_2O_2 -exposed organoid for final QC. Recapitulative table of scores for H_2O_2 -exposed organoid examples assessed through the Final QC. Individual scores obtained for each criterion and index of the QC are indicated, as well as minimal scores required for QC validation. Results of QC for each organoid are indicated as Passed / Failed QC.



В	H₂O₂ dose	Organoid number	Individual QC total score / 50	Median QC total score / 50	QC result	Step of exclusion (criterion and index)
			35 / 50	35 / 50		
•		#11	50			
	0%	#41	47	47	Passed	
	control	#57	47			
		#59	47			
		#21	45			
	0.1%	#37	48	46	Passed	
	0.1%	#55	45	40		
		#58	47			
		#8	45			
	0.25%	#36	45	44	Passed	
	0.2370	#48	43		1 43364	
		#50	45			
		#16	40			 D) Cytoarchitectures,
	0.5 0/	#30	12	4.5		 D1) Cellular density
	0.5%	#49	15	15	Failed	E) Cytotoxicity
		#52	24			E1) DNA damage
•		#23	14			C) Cellular
		#47	14	14	Failed	populations
	1%	#51	18			C2) Astrocytic
		#53	20			reactivity
•		#17	3	_	F 11 1	
		#20	6			 A) Morphology
	5%	#32	5	5	Failed	A2) Border integrity
		#46	6			1 12) 2 3 1 2 3 1 1 1 1 3 g 1 1 y

Fig. 4. Final QC scores obtained for all the ${\rm H_2O_2}$ -exposed cortical organoids. (**A**) Graphical representation of the final score distributions with median scores for each ${\rm H_2O_2}$ dose condition, as well as an indication of the QC passing or failure. Scores obtained by control organoids are significantly different from the scores obtained by the 1%- and 5%-treated conditions. Scores obtained by 0.1%-treated condition are also significantly different from the ones obtained by the 5%-treated condition. Kruskal-Wallis test followed by Dunn's post-hoc; n = 4; $p_{0\% \text{ vs. } 1\%} = 0.0353$; $p_{0\% \text{ vs. } 5\%} = 0.0007$; $p_{0.1\% \text{ vs. } 5\%} = 0.0049$. (**B**) Recapitulative table of individual final scores obtained by the H_2O_2 -exposed organoids, along with minimal scores required for QC validation. Median scores obtained per H_2O_2 dose conditions are also mentioned, as well as whether the organoids have passed or failed the QC. For those that have failed the QC, the scoring step at which they have been excluded is specified.

have been established for each criterion, and failure to meet these scores immediately classifies the organoids as low quality, excluding them from further evaluations (Fig. S1, Fig. 1B). If all the minimum scores are reached, additional thresholds incorporating multiple indices are applied to ensure a thorough quality assessment. As an example, for the morphology criterion, minimal scores required for the three indices are: 3/5 for density, 2/5 for border integrity, and 3/5 for absence of cysts, leading to a total of 8/15. However, the required minimal total score to pass the morphology criterion is not 8/15, but 9/15, implying that the evaluated organoid should not obtain minimal scores for each of the three indices, but should at least reach a higher score for one of them (Fig. 1B).

We demonstrated the effectiveness of our QC method through graded H₂O₂ exposures. Due to its ability to induce oxidative stress, eventually leading to cell death through apoptosis and necrosis at high doses^{62,63}, H,O, has been commonly used in organoid models to study oxidative damage-related mechanisms and to model aging and disease phenotypes^{87–90}. For the H₂O₂ exposure experiment, organoids were initially selected within a batch of cortical organoids using the Initial QC method. After H₂O₂ exposures, untreated and treated organoids were analyzed using the complete Final QC to assess post-treatment quality. Overall, the QC results demonstrated that only the untreated organoids and the organoids exposed to the lower doses of 0.1% and 0.25% H₂O₂ passed the QC, while those exposed to higher doses above 0.5% did not (Fig. 4). Median scores reflected the severity of H₂O₂ exposure, ranging from a very low QC score (5/50) for the highest dose to an elevated QC score (47/50) for controls, correlating with the degree of damage caused by the graded H2O2 exposures. Importantly, failures occurred at different steps of the hierarchical QC process: organoids exposed to 5%, 1% and 0.5% H₂O₂ were excluded during the first criterion (morphology), the third criterion (cellular composition), or the fourth criterion (cytoarchitecture), respectively. These results emphasize the necessity of a stepwise evaluation, as certain defects are detectable only through deeper cellular or subcellular analysis. Interestingly, organoids excluded early in the QC process were later found to exhibit high cytotoxicity levels in the final criterion, reinforcing the relevance of this hierarchical QC system. Taken together, these observations demonstrate the precision and reliability of the OC scoring system in differentiating organoid quality levels.

Although extensive characterization and validation are recommended for the development of novel differentiation protocols⁸⁶, including single-cell profiling with mapping to brain atlases or functional characterizations through electrophysiological activity recording, such analyses might be difficult to implement for routine QC. Our proposed QC framework is intentionally designed to be flexible and prioritizes widely adopted and cost-effective techniques, making it suitable for regular assessment of cerebral organoid quality across laboratories without the need for advanced or cost-prohibitive resources.

Interestingly, a few recent publications have demonstrated a growing interest in the use of morphological criteria as reliable non-invasive readouts for the characterization of cerebral organoids^{57–59}. Charles and colleagues have implemented a non-invasive quality control system relying on morphological criteria, enabling the classification of evaluated organoids in high- or low-quality categories for organoid pre-selection⁵⁹. Remarkably, they integrated brightfield image processing with machine learning tools, opening the way for automated quality assessment. However, this system is based solely on morphological observations and does not account for other important analysis criteria that may provide valuable insights beyond what is visible at the macro-scale. As our study demonstrates, using a scoring scale enables the detection of subtle variations that a binary classification might overlook. Additionally, the inclusion of parameters such as sphericity can be questioned, as many factors could be at the origin of shape variations independent of organoid quality. Serafini et al. have also developed a non-invasive imaging analysis method for cerebral organoid characterization, also based on brightfield images, and considering several morphological criteria⁵⁷. Using a 3D quantitative phase imaging technique, they assess parameters in a non-invasive manner, such as cellular content, cell morphologies, and rosettes. Similarly, Ikeda and colleagues have implemented a non-invasive morphological characterization of cerebral organoids combined with transcriptomic analyses⁵⁸. Interestingly, some analysis criteria are similar to those we selected, such as verification of transparency level and analysis of cystic structures⁵⁸. More broadly, an increasing number of studies rely on organoid analysis using brightfield imaging coupled with machine learning techniques, underscoring their growing significance in the field⁹¹⁻⁹⁴. Overall, morphological analysis serves as a valuable initial approach for assessing the quality and harvestability of cerebral organoids. Organoids with low QC scores often exhibit poor compactness, irregular borders or large cysts, making them unsuitable for harvesting and analysis. Our initial QC based on morphology reflects technical harvestability, while final quality is confirmed through more detailed, often invasive, analyses via our final QC.

While our proposed scoring system lays a foundation for organoid QC, there are still opportunities for further refinement and invasive techniques replacement. Notably, this scoring system can be applied manually, as proposed in this study, but could also be automated using image processing and machine learning analysis tools, offering flexibility, increased objectivity, faster execution, and higher throughput. Automated analysis could enable organoid images to be processed and partially scored through computational workflows, reducing variability in evaluations that might arise from individual interpretation. In particular, the automation could be envisaged primarily for criteria A) Morphology, based on brightfield images, as demonstrated by Charles and colleagues⁵⁹, and D) Cytoarchitecture, based on immunofluorescence images.

Additionally, incorporating other non-invasive criteria could significantly enhance the transferability of the scoring system for preclinical applications. These could include the detection of specific markers in the conditioned medium, such as lactate dehydrogenase activity measurement for cytotoxicity evaluation⁵⁶, apoptosis quantification, measurement of reactive oxygen species for oxidative stress analysis, and evaluation of metabolic activity. While numerous ready-to-use kits are available on the market for these analyses, particular attention must be paid to the normalization step, as these kits are typically designed to be normalized by cell number, which cannot be easily determined in 3D cultures⁵⁶. Other non-invasive methodologies also comprise label-free imaging techniques adapted for cerebral organoid characterization in 3D^{57,96}.

Although we confirm the presence of expected cell types in the evaluated organoids with the third criterion, it could also be valuable to ensure the absence of non-neural cells originating from non-neuroectodermal lineages during the differentiation^{1,50}, particularly through RNA sequencing, provided the feasibility of integrating such transcriptomic analyses into the routine QC workflow.

Regarding the last criterion, which addresses cellular viability and cytotoxicity assessments, we evaluated DNA damage through γ H2AX immunolabelling. However, other methods could also replace or complete this example, such as apoptosis detection via cleaved-caspase3 immunolabelling⁵⁴, TUNEL assay⁵³, or transcriptomic analyses evaluating pro- and anti-apoptotic markers like BAX and BCL2⁵².

After completing the morphological, structural, and cellular viability characterizations of our proposed QC approach, functional evaluations of the cerebral organoids could also be considered^{97,98}. This could involve assessing electrophysiological activity using calcium imaging¹³, patch-clamp², or microelectrode arrays (MEA) recordings^{51,99}, to confirm functional quality. Nonetheless, the use of these techniques with 3D organoids still poses some technical challenges, and their relevance depends on the specific applications^{97,98}.

Likewise, Organoid Intelligence (OI) is an emerging interdisciplinary field that integrates electrophysiological recordings from cerebral organoids with artificial intelligence-based analysis 100,101. Although still in its early stages and dependent on further refinement of organoid models 102, studies have shown that cerebral organoids can exhibit structured electrical activity, suggesting a potential for functional information processing. In this context, OI could enrich QC pipelines by offering insights into the functional maturity of neuronal networks. However, challenges remain, including technical limitations related to 3D cultures and variability in the onset and robustness of organoid activity. Overall, establishing reproducible functional readouts, such as electrical activity thresholds or machine-learning-based classification of network dynamics could considerably enhance scoring systems and may eventually support a new criterion of functional indices to complement existing QC features.

Ultimately, our framework provides flexibility, enabling the inclusion or exclusion of parameters based on the specific characteristics of the study (e.g., neurogenic niches, which could not be assessed here). However, to ensure consistency, it is crucial to define and validate thresholds through preliminary testing, especially when working with specific cell lines. Similarly, growth dynamics should be adjusted according to the number of cells used during 3D seeding.

Although our proposed QC methodology is specifically designed for the assessment of cortical organoids at 60 days, a key stage in their maturation process, our approach remains flexible and adaptable to different types of cerebral organoids and maturation timepoints. It may also serve as a QC framework for studies on disease modeling, where the scoring system could be adapted to focus on specific phenotypes critical for recapitulating pathological hallmarks, as well as in the context of neurodevelopmental toxicity evaluations, where it could facilitate systematic comparisons between exposed and non-exposed organoids. Additionally, reproducibility and scalability of cerebral organoids are central parameters to be considered both in fundamental and preclinical research. Beyond quality evaluation, this proposed scoring methodology can also indirectly reflect the intra- and inter-batch variability by analyzing the score dispersions among organoids within the same batch, and across different batches. In this regard, the QC scores can be used retrospectively to evaluate batch consistency. By addressing these evolving needs, this framework paves the way for more robust, reproducible, and versatile organoid-based research. Notably, it represents a critical step toward the much-needed collaborative effort to define and standardize quality expectations for different types of organoids. As the field moves toward increasingly complex models, such as assembloids. maintaining scientific rigor requires a shared foundation.

Methods

HiPSC culture and maintenance

Human induced Pluripotent Stem Cells (hiPSCs) were generated by reprogramming BJ primary foreskin fibroblasts obtained from ATCC (CRL-2522), using non-integrative Sendai virus vectors following the manufacturer's instructions (A16517, ThermoFisher Scientific). Pluripotency was confirmed by identifying specific pluripotency markers through Reverse Transcriptase-Polymerase Chain Reaction (RT-PCR), and regular tests were conducted to verify the absence of mycoplasma. The culture and maintenance of hiPSCs were performed as previously reported^{21,22,56}. Briefly, hiPSCs were maintained on Geltrex-coated cell culture plates (A1569601, Gibco) and cultured in mTeSR Plus medium (100–0276, STEMCELL Technologies) supplemented with 1% Penicillin/Streptomycin (P/S) (15140122, Gibco), at 37 °C in a 5%-enriched CO $_2$ atmosphere. hiPSCs were passaged upon reaching 50–70% confluency using 0.02% ethylenediaminetetraacetic acid (EDTA) treatment (E8008, Sigma-Aldrich).

Generation and culture of cerebral cortical organoids

Cerebral cortical organoids were generated as previously reported 56 , from a protocol adapted from methods described by Xiang et al. $^{4.5}$ relying on dorsal forebrain-regionalized differentiation. On day 0, hiPSCs were detached using 0.02% EDTA treatment and dissociated with Accutase (AT-104, STEMCELL Technologies) to obtain a single-cell suspension. These cells were seeded in V-bottom cell-repellent 96-well plates (651970, Greiner Bio-One) at a density of 20,000 cells/well in neural induction medium containing Dulbecco's Modified Eagle Medium/Nutrient Mixture F-12, GlutaMAX supplement (DMEM/F-12, 10565018, Gibco), 15% (v/v) KnockOut Serum Replacement (KOSR, 10828010, Gibco), 1% Minimum Essential Medium-Non-Essential Amino Acids (MEM-NEAA, 1140035, Gibco), 1% P/S, 100 nM LDN-193,189 (72147, STEMCELL Technologies), 10 μ M SB-431,542 (72232, STEMCELL Technologies), 2 μ M XAV-939 (X3004, Sigma-Aldrich), 100 μ M μ 9-mercaptoethanol (21985023, Gibco), and supplemented with 5% Fetal Bovine Serum (FBS, 10270106, Gibco) and 50 μ M Y-27632 (72304, STEMCELL Technologies). On day 2, embryoid bodies (EBs) were collected and transferred into 24-well suspension cell culture plates (144530, Nunc). The neural induction medium was renewed every two days

until day 10, with FBS removed from day 2, and Y-27632 removed from day 4. From day 10 to day 18, EBs were cultured in differentiation medium without vitamin A, containing DMEM/F-12:NeuroBasal Medium (21103049, Gibco) at 1:1 ratio, supplemented with 0.5% (v/v) MEM-NEAA, 1% P/S, 0.5% N2 supplement $100\times(17502-048, Gibco)$, 1% B-27 supplement minus vitamin A (12587010, Gibco), 1% HEPES solution (H0887, Sigma-Aldrich), 0.025% human insulin (19278-5 mL, Sigma-Aldrich), and 50 μ M β -mercaptoethanol. From day 18, EBs were cultured in a differentiation medium with vitamin A, following the same composition as the previously described medium, but replacing the B-27 supplement minus vitamin A, with B-27 supplement with vitamin A (17504044, Gibco), and supplemented with 20 ng/mL BDNF (78005, STEMCELL Technologies), 200 μ M ascorbic acid (A9290225G, Sigma-Aldrich), and 200 μ M cAMP (73886, STEMCELL Technologies). Cortical organoids were cultured in 24-well plates with 500 μ L of culture medium renewed every two days from day 2 to day 28. After day 28, the medium volume was increased to 1 mL and renewed once a week. Organoids were cultured under agitation (80 rpm) at 37 °C, in a 5%-enriched CO₂ atmosphere.

H₂O₂ exposures on cortical organoids

Cortical organoids were exposed on day 61 of culture to hydrogen peroxide (H_2O_2) (1.07209.0250, Supelco) diluted in differentiation medium with vitamin A, at several doses (0.1%, 0.25%, 0.5%, 1% and 5%) during 30 min at 37 °C. After exposure, cortical organoids were washed once with fresh culture medium to remove excess H_2O_2 , were maintained in culture for 7 days, and were fixed on day 68.

Quality control of cortical organoids: scoring system

A multi-criteria scoring system was developed for the QC of 60-day cortical organoids (Fig. 1 and Fig. S1). Briefly, each QC criterion is subdivided into indices, which are scored on a scale ranging from 0 (low quality) to 5 (high quality) to assess cortical organoid quality (Fig. S1). To facilitate the evaluation process, criteria are hierarchically organized, with priority given to non-invasive and critical parameters (Fig. 1A). Minimum score thresholds are defined for each individual index (Fig. 1B), and failure to meet any of these minimal scores results in immediate classification as low quality, and exclusion from further analysis (Fig. 1A). Through this design, the QC framework prioritizes and provides more weight to early-stage criteria. Minimum scores were defined not only at the level of individual indices, but also across each criterion. Therefore, even if an organoid meets the minimum scores for all indices within a given criterion, it may still be excluded if the total criterion score falls below the required threshold (Fig. 1A, B).

For the QC scoring, a detailed description (Fig. S1) outlines expected values and scoring thresholds for each index. Additionally, a summary table with the minimum scores required to pass the QC for each criterion is presented (Fig. 1B). Based on their individual QC scores obtained, cortical organoids are classified into "QC passed" or "QC failed" categories, with the specification of the failed scoring step for any organoid that did not pass the QC. More precisely, the scoring approach is tailored to be usable both for pre- and post-study, referred to as Initial QC and Final QC, respectively.

Initial quality control

In the pre-study phase, the first two non-invasive criteria, A (Morphology) and B (Size and Growth Profile), are evaluated across a batch of cortical organoids, to identify those suitable for inclusion in the subsequent study. The morphology of the organoids is assessed based on their color, density, compactness, border integrity, as well as depending on the absence or presence of cysts. In addition, organoid sizes and growth profiles are monitored to ensure they remain within expected growth ranges.

Final quality control

In the post-study phase, all five criteria – A to E – are used to thoroughly validate organoid quality. This includes additional evaluations of cellular populations (criterion C), where the presence of the three expected cell types (neurons, astrocytes, neural progenitors) and astrocytic reactivity are analyzed, as well as assessments of the cytoarchitectural organization (criterion D), including cell density, proportion of cell-less regions, border integrity, presence of neurogenic areas, and occurrence of internal cysts. Finally, cell viability and cytotoxic markers (criterion E) are evaluated, with a focus on DNA damage, to ensure organoids have maintained low cytotoxicity levels throughout the study.

Longitudinal monitoring of cortical organoid morphology and growth evolution

For cortical organoid morphology and growth profile monitoring over time, brightfield images of the organoids were acquired at regular timepoints during the culture (D+2, D+9, D+16, D+23, D+30, D+33, D+40, D+48, D+54 and D+61), using a DM IL LED Inverted Laboratory Microscope (Leica Microsystems) (5X). To assess the organoid size, the surface area of the organoid was measured from the brightfield images on FIJI/ImageJ software, version $1.54f^{103}$.

Immunohistochemistry

Cortical organoids were fixed in 4% paraformaldehyde (11699408, Q Path) for 2 h at room temperature (RT) under smooth agitation, followed by three washes of 10 min with Phosphate Buffered Saline solution (PBS) (18912-014, Gibco) at RT under smooth agitation, and immersed in 30% (v/v) sucrose (S9378, Sigma-Aldrich) dissolved in PBS for 48 h at 4 °C. The organoids were then transferred in a solution composed of 7.5% (v/v) gelatin (G9391, Sigma-Aldrich) and 15% (v/v) sucrose dissolved in PBS for 1 h at 37 °C, before being embedded in this solution for 15 min at 4 °C. Embedded organoids were then snap-frozen in isopentane (M32631, Sigma-Aldrich) and stored at -80 °C until use. Frozen organoids were sectioned in slices of 20 µm thickness using a cryostat (CM1850 UV, Leica Biosystems). For the immunofluorescent staining, organoid slices were

Primary antibody	Host and isotype	Supplier and reference	Dilution
Anti-SOX2	Mouse IgG1	Proteintech, 66477-1-Ig	1:500
Anti-TUBB3	Mouse IgG2a	Biolegend, 801,202	1:500
Anti-GFAP	Rabbit IgG	Dako, Z0334	1:1000
Anti-γH2AX	Mouse IgG1	Sigma-Aldrich, 05-636	1:500
Secondary antibody	Host	Supplier and reference	Dilution
Alexa Fluor [*] Cy3 anti-mouse IgG1	Goat	Jackson ImmunoResearch, 115- 165-205	1:500
Alexa Fluor [*] 488 anti-mouse IgG2a	Goat	Jackson ImmunoResearch, 115- 547-186	1:500
Alexa Fluor [*] 647 anti-rabbit IgG	Goat	Jackson ImmunoResearch, 111- 605-144	1:500
Alexa Fluor [*] 488 anti-mouse IgG1	Goat	Jackson ImmunoResearch, 115- 547-185	1:500

Table 2. Primary and secondary antibodies used for immunofluorescent stainings.

permeabilized and blocked with a solution containing 0.2% Triton X-100 (T-9284, Sigma-Aldrich), 3% bovine serum albumin (BSA, A2153, Sigma-Aldrich), and 1% normal goat serum (NGS, G9023, Sigma-Aldrich) in PBS for 1 h at RT. Then, the slices were incubated with primary antibodies diluted in the blocking solution at 4 °C overnight in a humidified chamber and were washed with 0.2% Triton in PBS three times. Then, organoid slices were incubated with secondary antibodies and 4′,6-diamidino-2-phenylindole (DAPI, dilution 1:1000) for 1 h at RT in a dark humidified chamber and were washed three times with 0.2% Triton in PBS. The slices were mounted using ProLong Gold Antifade Mountant (11539306, Invitrogen), and observed under a Leica THUNDER microscope (THUNDER Imager 3D Assay, Leica Microsystems) with the Leica Application Suite X software version 3.8.2.27713. Primary and secondary antibodies used are listed in Table 2.

Image-based quantifications of cellular density and cell-less regions

Cellular density was calculated based on DAPI positive surface, without considering cell-less zones ("holes") since this second parameter was considered in the subsequent index. Both quantifications of cellular density and cell-less regions relied on determination of DAPI positive surface and were normalized to the total surface area of the organoid slice. Briefly, the DAPI positive surface was determined using the "Adjust Threshold" function of FIJI/ImageJ. For the cellular density, the threshold was adjusted to correspond with the DAPI labelling, while for the cell-less areas, the threshold was increased to cover the entire surface except the cell-less regions/holes. Estimation of cell number was calculated based on DAPI positive surface, considering an average nucleus area of $80~\mu m^2$.

Image-based quantification of GFAP positive surface expression

Glial Fibrillary Acidic Protein (GFAP) positive surface expression was calculated using the "Adjust Threshold" function on FIJI/ImageJ, as previously described in this section, and normalized to the total DAPI positive surface area of the cryosection.

Image-based quantification of yH2AX marker and comparison with a positive control

Quantification was conducted by counting χ H2AX punctate and by normalizing to the DAPI positive surface expression, across several sections of individual organoids (n=2–3 slices per organoid, n=4 organoids per condition). Images were first binarized on FIJI/ImageJ, then the "Analyze Particles" function was applied with the following parameters: Size (micron2): 15-infinity, Circularity: 0.00–1.00. To statistically compare the maximal χ H2AX immunolabelling in cerebral organoids with positive controls, the standard deviation of the positive controls was first calculated. Then, the difference between the mean value of the positive controls and the value for the organoids was determined. Finally, this difference was expressed as a ratio relative to the standard deviation of the positive controls.

Experimental design, randomization and statistical analysis

The QC framework – including criteria, scores, thresholds, and representative organoid examples illustrating each score (Fig. S1) – was developed based on data and images collected from a large number of in-house studies using cortical organoids derived from healthy donor-iPSCs. These studies, conducted over the past four years, encompassed more than 30 independent organoid batches and a total of more than 1200 individual organoids that were characterized. This extensive dataset provided sufficient perspective to discriminate between high- and low-quality organoids, and intermediate stages, as well as to determine which criteria were the most critical in the QC system structure.

Cortical organoids used for the H_2O_2 exposure experiment were selected based on their Initial QC scores (harvestability) and were randomly distributed across experimental groups before H_2O_2 exposures (n=4 per

group). Images and data from the exposed organoids were collected and coded by one experimenter, then blindly evaluated for QC by a second experimenter.

Statistical analyses were conducted using GraphPad Prism 10 (version 10.5.0). Since residuals were not normally distributed (Shapiro-Wilk test), non-parametric tests were used (Friedman and Kruskal-Wallis), followed by Dunn's post hoc correction for multiple comparisons.

Data availability

The datasets generated during and/or analysed during the current study are available from the corresponding author on reasonable request.

Received: 29 April 2025; Accepted: 31 July 2025

Published online: 11 August 2025

References

- Qian, X., Song, H. & Ming, G. L. Brain organoids: advances, applications and challenges. Development 146, dev166074. https://doi.org/10.1242/dev.166074 (2019).
- Pasca, A. M. et al. Functional cortical neurons and astrocytes from human pluripotent stem cells in 3D culture. Nat. Methods. 12, 671–678. https://doi.org/10.1038/nmeth.3415 (2015).
- Susaimanickam, P. J., Kiral, F. R. & Park, I. H. Region specific brain organoids to study neurodevelopmental disorders. Int. J. Stem Cells. 15, 26–40. https://doi.org/10.15283/IJSC22006 (2022).
- 4. Xiang, Y. et al. Fusion of regionally-specified hPSC-derived organoids models human brain development and interneuron migration. Cell. Stel Cell. 21, 383–398. https://doi.org/10.1016/j.stem.2017.07.007.Fusion (2017).
- Xiang, Y. et al. hESC-derived thalamic organoids form reciprocal projections when fused with cortical organoids. Cell. Stem Cell. 24, 487–497. https://doi.org/10.1016/j.stem.2018.12.015.hESC-derived (2019).
- Velasco, S. et al. Individual brain organoids reproducibly form cell diversity of the human cerebral cortex. *Nature* 570, 523–527. https://doi.org/10.1038/s41586-019-1289-x (2019).
- 7. Muguruma, K. et al. Self-organization of polarized cerebellar tissue in 3D culture of human pluripotent stem cells. *Cell. Rep.* 10, 537–550. https://doi.org/10.1016/j.celrep.2014.12.051 (2015).
- 8. Sakaguchi, H. et al. Generation of functional hippocampal neurons from self-organizing human embryonic stem cell-derived dorsomedial telencephalic tissue. *Nat. Commun.* 6. https://doi.org/10.1038/ncomms9896 (2015).
- Qian, X. et al. Brain-Region-Specific organoids using Mini-bioreactors for modeling ZIKV exposure. Cell 165, 1238–1254. https://doi.org/10.1016/j.cell.2016.04.032 (2016).
- Zagare, A., Gobin, M., Monzel, A. S. & Schwamborn, J. C. A robust protocol for the generation of human midbrain organoids. STAR Protoc. 2. https://doi.org/10.1016/j.xpro.2021.100524 (2021).
- 11. Zivko, C. et al. IPSC-derived hindbrain organoids to evaluate Escitalopram oxalate treatment responses targeting neuropsychiatric symptoms in alzheimer's disease. *Mol. Psychiatry.* 29, 3644–3652. https://doi.org/10.1038/s41380-024-02629-y (2024).
- Pellegrini, L. et al. Human CNS barrier-forming organoids with cerebrospinal fluid production. Science 369. https://doi.org/10.1 126/SCIENCE.AAZ5626 (2020).
- Lancaster, M. A. et al. Cerebral organoids model human brain development and microcephaly. Nature 501, 373–379. https://doi. org/10.1038/nature12517 (2013).
- Wu, X. et al. Recent advances in Three-Dimensional stem cell culture systems and applications. Stem Cells Int. 2021, 9477332. https://doi.org/10.1155/2021/9477332 (2021).
- Chiaradia, I. & Lancaster, M. A. Brain organoids for the study of human neurobiology at the interface of in vitro and in vivo. *Nat. Neurosci.* 23, 1496–1508. https://doi.org/10.1038/s41593-020-00730-3 (2020).
- 16. Amiri, A. et al. Transcriptome and epigenome landscape of human cortical development modeled in organoids. *Science* 362, eaat6720 (2018). https://doi.org/10.1126/science.aat6720
- 17. Tang, X. Y. et al. DSCAM/PAK1 pathway suppression reverses neurogenesis deficits in iPSC-derived cerebral organoids from patients with down syndrome. J. Clin. Invest. 131, e135763. https://doi.org/10.1172/JCI135763 (2021).
- 18. Xu, R. et al. OLIG2 drives abnormal neurodevelopmental phenotypes in human iPSC-Based organoid and chimeric mouse
- models of down syndrome. *Cell. Stem Cell.* **24**, 908–926. https://doi.org/10.1016/j.stem.2019.04.014.OLIG2 (2019).

 19. Alić, I. et al. Patient-specific Alzheimer-like pathology in trisomy 21 cerebral organoids reveals BACE2 as a gene dose-sensitive
- AD suppressor in human brain. *Mol. Psychiatry.* 26, 5766–5788. https://doi.org/10.1038/s41380-020-0806-5 (2021).

 20. Bian, S. et al. Genetically engineered cerebral organoids model brain tumour formation. *Nat. Methods.* 15, 631–639. https://doi.org/10.1038/s41592-018-0070-7.Genetically (2018).
- Nassor, F. et al. Long term gene expression in human induced pluripotent stem cells and cerebral organoids to model a neurodegenerative disease. Front. Cell. Neurosci. 14, 14. https://doi.org/10.3389/fncel.2020.00014 (2020).
- 22. Pavoni, Š. et al. Small-molecule induction of Aβ-42 peptide production in human cerebral organoids to model alzheimer's disease associated phenotypes. *PLoS One.* 13, e0209150. https://doi.org/10.1371/journal.pone.0209150 (2018).
- 23. Kim, H. et al. Modeling G2019S-LRRK2 sporadic parkinson's disease in 3D midbrain organoids. Stem Cell. Rep. 12, 518-531. https://doi.org/10.1016/j.stemcr.2019.01.020 (2019).
- Groveman, B. R. et al. Sporadic Creutzfeldt-Jakob disease prion infection of human cerebral organoids. *Acta Neuropathol. Commun.* 7, 90. https://doi.org/10.1186/s40478-019-0742-2 (2019).
- 25. Giorgi, C. et al. Brain organoids: A Game-Changer for drug testing. *Pharmaceutics* https://doi.org/10.3390/pharmaceutics16040443
- (2024).
 26. Zhou, J. Q. et al. Brain organoids are new tool for drug screening of neurological diseases. *Neural Regen Res.* 18, 1884–1889. https://doi.org/10.4103/1673-5374.367983 (2023).
- 27. Saglam-Metiner, P. et al. Humanized brain organoids-on-chip integrated with sensors for screening neuronal activity and neurotoxicity. *Microchimica Acta* 2024. **191** (1 191), 1–25. https://doi.org/10.1007/S00604-023-06165-4 (2024).
- 28. Cui, K. et al. Neurodevelopmental impairment induced by prenatal valproic acid exposure shown with the human cortical organoid-on-a-chip model. *Microsyst. Nanoeng.* 6 https://doi.org/10.1038/s41378-020-0165-z (2020).
- Zang, Z. et al. Valproic acid exposure decreases neurogenic potential of outer radial glia in human brain organoids. Front. Mol. Neurosci. 15 https://doi.org/10.3389/fnmol.2022.1023765 (2022).
- 30. Meng, Q. et al. Human forebrain organoids reveal connections between valproic acid exposure and autism risk. *Transl Psychiatry*. 12, 130. https://doi.org/10.1038/s41398-022-01898-x (2022).
- 31. Rhinn, M. et al. Aberrant induction of p19Arf-mediated cellular senescence contributes to neurodevelopmental defects. *PLoS Biol.* **20** https://doi.org/10.1371/journal.pbio.3001664 (2022).
- 32. Yokoi, R. et al. Contraindicated drug responses in Dravet syndrome brain organoids utilizing micro electrode array assessment methods. *Organoids* 2, 177–191. https://doi.org/10.3390/organoids2040014 (2023).

- 33. TaklaTN et al. A shared pathogenic mechanism for valproic acid and SHROOM3 knockout in a brain organoid model of neural tube defects. *Cells* 12. https://doi.org/10.3390/cells12131697 (2023).
- 34. Tidball, A. M. et al. Deriving early single-rosette brain organoids from human pluripotent stem cells. Stem Cell. Rep. 18, 2498–2514. https://doi.org/10.1016/j.stemcr.2023.10.020 (2023).
- 35. Lee, J. H., Shaker, M. R., Park, S. H. & Sun, W. Transcriptional signature of valproic Acid-Induced neural tube defects in human spinal cord organoids. *Int. J. Stem Cells.* 16, 385–393. https://doi.org/10.15283/IJSC23012 (2023).
- 36. Wang, Y., Wang, L., Zhu, Y. & Qin, J. Human brain organoid-on-a-chip to model prenatal nicotine exposure. Lab. Chip. 18, 851-860. https://doi.org/10.1039/c7lc01084b (2018).
- 37. Ao, Z. et al. One-Stop microfluidic assembly of human brain organoids to model prenatal cannabis exposure. *Anal. Chem.* **92**, 4630–4638. https://doi.org/10.1021/acs.analchem.0c00205 (2020).
- 38. Abdulla, A. et al. A multichannel microfluidic device for revealing the neurotoxic effects of bisphenol S on cerebral organoids under low-dose constant exposure. *Biosens. Bioelectron.* **267**, 116754. https://doi.org/10.1016/J.BIOS.2024.116754 (2025).
- Cao, Y. et al. Modeling early human cortical development and evaluating neurotoxicity with a forebrain organoid system. *Environ. Pollut.* 337 https://doi.org/10.1016/j.envpol.2023.122624 (2023).
- 40. Hu, D. et al. Establishment of human cerebral organoid systems to model early neural development and assess the central neurotoxicity of environmental toxins. Neural Regen Res. 20, 242–252. https://doi.org/10.4103/nrr.nrr-d-23-00928 (2025).
- Chen, S. et al. Toxic effects and mechanisms of nanoplastics on embryonic brain development using brain organoids model. Sci. Total Environ. https://doi.org/10.1016/j.scitotenv.2023.166913 (2023). 904:.
- 42. Yao, H. et al. Buprenorphine and methadone differentially alter early brain development in human cortical organoids.
- Neuropharmacology 239. https://doi.org/10.1016/j.neuropharm.2023.109683 (2023).
 Liu, Z. et al. Transcriptomic profiling of Tetrodotoxin-Induced neurotoxicity in human cerebral organoids. Mar. Drugs. 21, 588. https://doi.org/10.3390/md21110588 (2023).
- 44. Tian, C. et al. Engineering human midbrain organoid microphysiological systems to model prenatal PFOS exposure. *Sci. Total Funitors* **947**, 174478, https://doi.org/10.1016/J.SCITOTENV.2024.174478 (2024)
- Environ. 947, 174478. https://doi.org/10.1016/J.SCITOTENV.2024.174478 (2024).
 Acharya, P. et al. Dynamic culture of cerebral organoids using a pillar/perfusion plate for the assessment of developmental neurotoxicity. Biofabrication 17, 015001. https://doi.org/10.1088/1758-5090/ad867e (2024).
- Castiglione, H. et al. Human brain Organoids-on-Chip: advances, challenges, and perspectives for preclinical applications. *Pharmaceutics* 14, 2301. https://doi.org/10.3390/pharmaceutics14112301 (2022).
- Giandomenico, S. L., Sutcliffe, M. & Lancaster, M. A. Generation and long-term culture of advanced cerebral organoids for studying later stages of neural development. *Nat. Protoc.* 16, 579–602. https://doi.org/10.1038/s41596-020-00433-w (2021).
- Lancaster, M. A. & Knoblich, J. A. Generation of cerebral organoids from human pluripotent stem cells. Nat. Protoc. 9, 2329–2340. https://doi.org/10.1038/nprot.2014.158.Generation (2014).
- 49. Kang, Y. J. & Cho, H. Human brain organoids in alzheimer's disease. *Organoid* 1, e5. https://doi.org/10.51335/organoid.2021.1.e5
- 50. Quadrato, G. et al. Cell diversity and network dynamics in photosensitive human brain organoids. *Nature* **545**, 48–53. https://doi.org/10.1038/nature22047 (2017).
- 51. Schröter, M. et al. Functional imaging of brain organoids using high-density microelectrode arrays. MRS Bull. 47, 530–544.
- https://doi.org/10.1557/s43577-022-00282-w (2022).

 52. Basu, A. & Haldar, S. The relationship between Bcl2, Bax and p53: consequences for cell cycle progression and cell death. *Mol.*
- Hum. Reprod. 4, 1099–1109. https://doi.org/10.1093/molehr/4.12.1099 (1998).

 53. Loo, D. T. In situ detection of apoptosis by the TUNEL assay: an overview of techniques. Methods Mol. Biol. 682, 3–13. https://d
- oi.org/10.1007/978-1-60327-409-8_1 (2011).
 54. Bressenot, A. et al. Assessment of apoptosis by immunohistochemistry to active Caspase-3, active Caspase-7, or cleaved PARP in monolayer cells and spheroid and subcutaneous xenografts of human carcinoma. *J. Histochem. Cytochem.* 57, 289–300. https://d
- oi.org/10.1369/jhc.2008.952044 (2009).

 55. Podhorecka, M., Skladanowski, A. & Bozko, P. H2AX phosphorylation: its role in DNA damage response and cancer therapy. *J. Nucleic Acids.* 2010, 920161. https://doi.org/10.4061/2010/920161 (2010).
- Castiglione, H. et al. Development and optimization of a lactate dehydrogenase assay adapted to 3D cell cultures. Organoids 3, 113–125. https://doi.org/10.3390/organoids3020008 (2024).
- 57. Serafini, C. É. et al. Non-invasive label-free imaging analysis pipeline for in situ characterization of 3D brain organoids. *Sci. Rep.* 14, 22331. https://doi.org/10.1038/s41598-024-72038-2 (2024).
- 58. Ikeda, M. et al. Validation of non-destructive morphology-based selection of cerebral cortical organoids by paired morphological and single-cell RNA-seq analyses. Stem Cell. Rep. 19, 1635–1646. https://doi.org/10.1016/j.stemcr.2024.09.005 (2024).
- 59. Charles, S. et al. Non-Invasive quality control of organoid cultures using mesofluidic CSTR bioreactors and High-Content imaging. Adv. Mater. Technol. 10. https://doi.org/10.1002/admt.202400473 (2025).
- Temple, J., Velliou, E., Shehata, M. & Lévy, R. Current strategies with implementation of three-dimensional cell culture: The challenge of quantification. *Interface Focus.* 12. https://doi.org/10.1098/rsfs.2022.0019 (2022).
- 61. Di Lullo, E. & Kriegstein, A. R. The use of brain organoids to investigate neural development and disease. *Nat. Rev. Neurosci.* 18, 573–584. https://doi.org/10.1038/nrn.2017.107 (2017).
- 62. Chidawanyika, T. & Supattapone, S. Hydrogen Peroxide-induced cell death in mammalian cells. *J. Cell. Signal.* 2, 206–211. https://doi.org/10.33696/signaling.2.052 (2021).
- 63. Chen, L. et al. Hydrogen peroxide-induced neuronal apoptosis is associated with Inhibition of protein phosphatase 2A and 5, leading to activation of MAPK pathway. *Int. J. Biochem. Cell. Biology.* 41, 1284–1295. https://doi.org/10.1016/j.biocel.2008.10.029 (2009).
- 64. Cho, A. N. et al. Microfluidic device with brain extracellular matrix promotes structural and functional maturation of human brain organoids. *Nat. Commun.* 12, 4730. https://doi.org/10.1038/s41467-021-24775-5 (2021).
- 65. Wang, Y. et al. Engineering stem cell-derived 3D brain organoids in a perfusable organ-on-a-chip system. RSC Adv. 8, 1677–1685. https://doi.org/10.1039/c7ra11714k (2018).
- Karzbrun, E. et al. Human brain organoids on a chip reveal the physics of folding. Nat. Phys. 14, 515–522. https://doi.org/10.103 8/s41567-018-0046-7 (2018).
- 67. Cecen, B. et al. Biosensor integrated brain-on-a-chip platforms: progress and prospects in clinical translation. *Biosens. Bioelectron.* 225. https://doi.org/10.1016/j.bios.2023.115100 (2023).
- Grün, C., Altmann, B. & Gottwald, E. Advanced 3d cell culture techniques in micro-bioreactors, part I: A systematic analysis of the literature published between 2000 and 2020. Processes 8, 1656. https://doi.org/10.3390/pr8121656 (2020).
- Altmann, B., Grün, C., Nies, C. & Gottwald, E. Advanced 3D cell culture techniques in Micro-Bioreactors, part II: systems and applications. *Processes* 9, 21. https://doi.org/10.3390/pr9010021 (2020).
- 70. Qian, X. et al. Generation of human brain region–specific organoids using a miniaturized spinning bioreactor. *Nat. Protoc.* 13, 565–580. https://doi.org/10.1038/nprot.2017.152 (2018).
- 71. Suong, D. N. A., Imamura, K., Kato, Y. & Inoue, H. Design of neural organoids engineered by mechanical forces. *IBRO Neurosci. Rep.* 16, 190–195. https://doi.org/10.1016/J.IBNEUR.2024.01.004 (2024).
- 72. Acharya, P. et al. Brain organoids: A revolutionary tool for modeling neurological disorders and development of therapeutics. Biotechnol. Bioeng. 121, 489–506. https://doi.org/10.1002/BIT.28606 (2024).

- 73. Garreta, E. et al. Rethinking organoid technology through bioengineering. Nat. Mater. 20, 145–155. https://doi.org/10.1038/s415 63-020-00804-4 (2021).
- Hofer, M. & Lutolf, M. P. Engineering organoids. Nat. Rev. Mater. 6, 402–420. https://doi.org/10.1038/s41578-021-00279-y (2021).
- 75. Cadena, M. A. et al. A 3D bioprinted cortical organoid platform for modeling human brain development. *Adv. Healthc. Mater.* 13, e2401603. https://doi.org/10.1002/adhm.202401603 (2024).
- 76. Roth, J. G. et al. Spatially controlled construction of assembloids using Bioprinting. *Nat. Commun.* 14, 4346. https://doi.org/10.1038/s41467-023-40006-5 (2023).
- 77. Kistemaker, L., van Bodegraven, E. J., de Vries, H. E. & Hol, E. M. Vascularized human brain organoids: current possibilities and prospects. *Trends Biotechnol.* 43, 1275–1285. https://doi.org/10.1016/J.TIBTECH.2024.11.021 (2025).
- Tan, S. Y., Feng, X., Cheng, L. K. W. & Wu, A. R. Vascularized human brain organoid on-chip. *Lab. Chip.* 23, 2693–2709. https://doi.org/10.1039/d2lc01109c (2023).
- 79. Zhang, W. et al. Microglia-containing human brain organoids for the study of brain development and pathology. *Mol. Psychiatry*. 28, 96–107. https://doi.org/10.1038/S41380-022-01892-1 (2023).
- Ormel, P. R. et al. Microglia innately develop within cerebral organoids. Nat. Commun. 2018, 9:1 9:1–14 (2018). https://doi.org/1 0.1038/s41467-018-06684-2
- 81. Fagerlund, I. et al. Microglia-like cells promote neuronal functions in cerebral organoids. *Cells* 11, 124. https://doi.org/10.3390/CELLS11010124/S1 (2022).
- 82. Abud, E. M. et al. iPSC-derived human microglia-like cells to study neurological diseases. Neuron 94, 278. https://doi.org/10.1016/J.NEURON.2017.03.042 (2017).
- 83. Pagliaro, A., Artegiani, B. & Hendriks, D. Emerging approaches to enhance human brain organoid physiology. *Trends Cell. Biol.*
- 35, 483–499. https://doi.org/10.1016/J.TCB.2024.12.001 (2025).
 84. Miura, Y. et al. Engineering brain assembloids to interrogate human neural circuits. *Nat. Protoc.* 17, 15–35. https://doi.org/10.10 38/s41596-021-00632-z (2022).
- Paşca, S. P. et al. A nomenclature consensus for nervous system organoids and assembloids. Nature 609, 907–910. https://doi.org/10.1038/s41586-022-05219-6 (2022).
- 86. Pasca, S. P. et al. A framework for neural organoids, assembloids and transplantation studies. *Nature* https://doi.org/10.1038/s41 586-024-08487-6 (2024).
- Hossain, M. K., Kim, H. R. & Chae, H. J. Aging phenotype in AD brain organoids: track to success and challenges. Ageing Res. Rev. 96 https://doi.org/10.1016/j.arr.2024.102256 (2024).
- Seo, W. M. et al. Modeling axonal regeneration by changing cytoskeletal dynamics in stem cell-derived motor nerve organoids. Sci. Rep. 12. https://doi.org/10.1038/s41598-022-05645-6 (2022).
- Sci. Rep. 12. https://doi.org/10.1038/s41598-022-05645-6 (2022).
 Kawada, J. et al. Generation of a motor nerve organoid with human stem Cell-Derived neurons. Stem Cell. Rep. 9, 1441–1449. https://doi.org/10.1016/j.stemcr.2017.09.021 (2017).
- 90. Csukovich, G. et al. The intricacies of inflammatory bowel disease: A preliminary study of redox biology in intestinal organoids. Organoids 2, 156–164. https://doi.org/10.3390/organoids2030012 (2023).
- Organoias 2, 156–164. https://doi.org/10.3590/organoias2030012 (2025).

 91. Park, T. et al. Development of a deep learning based image processing tool for enhanced organoid analysis. Sci. Rep. 13. https://doi.org/10.1038/s41598-023-46485-2 (2023).
- 92. Matthews, J. M. et al. OrganoID: A versatile deep learning platform for tracking and analysis of single-organoid dynamics. *PLoS Comput. Biol.* 18 https://doi.org/10.1371/journal.pcbi.1010584 (2022).
- 93. Powell, R. T. et al. DeepOrganoid: A Brightfield cell viability model for screening matrix-embedded organoids. *SLAS Discovery*.
- 27, 175–184. https://doi.org/10.1016/j.slasd.2022.03.004 (2022).
 94. Deben, C. et al. Development and validation of the normalized organoid growth rate (NOGR) metric in Brightfield imaging-based assays. *Commun. Biol.* 7 https://doi.org/10.1038/s42003-024-07329-5 (2024).
- Saglam-Metiner, P. et al. Spatio-temporal dynamics enhance cellular diversity, neuronal function and further maturation of human cerebral organoids. Commun. Biol. 2023, 6:1 6:1–18. (2023). https://doi.org/10.1038/s42003-023-04547-1
- 96. Bruno, G. et al. Label-Free detection of biochemical changes during cortical organoid maturation via Raman spectroscopy and machine learning. *Anal. Chem.* https://doi.org/10.1021/acs.analchem.4c05661 (2025).
- 97. Tasnim, K. & Liu, J. Emerging bioelectronics for brain organoid electrophysiology. J. Mol. Biol. 434, 167165. https://doi.org/10.1016/i.imb.2021.167165 (2022).
- Passaro, A. P. & Stice, S. L. Electrophysiological analysis of brain organoids: current approaches and advancements. Front. Neurosci. 14, 1–13. https://doi.org/10.3389/fnins.2020.622137 (2021).
- Giandomenico, S. L. et al. Cerebral organoids at the air-liquid interface generate diverse nerve tracts with functional output. *Nat. Neurosci.* 22, 669–679. https://doi.org/10.1038/s41593-019-0350-2 (2019).
- 100. Hartung, T., Morales Pantoja, I. E. & Smirnova, L. Brain organoids and organoid intelligence from ethical, legal, and social points
- of view. Front. Artif. Intell. 6, 1307613. https://doi.org/10.3389/FRAI.2023.1307613/XML (2023).

 101. Smirnova, L. et al. Organoid intelligence (OI): the new frontier in biocomputing and intelligence-in-a-dish. Front. Sci. 1, 1017235. https://doi.org/10.3389/FSCI.2023.1017235 (2023).
- 102. Nestor, M. W., Wilson, R. L., Nestor, M. W. & Wilson, R. L. Assessing the utility of organoid intelligence: Scientific and ethical perspectives. *Organoids* 4, 9 (2025). https://doi.org/10.3390/ORGANOIDS4020009
- 103. Schindelin, J. et al. Fiji: an open-source platform for biological-image analysis. *Nat. Methods.* **9**, 676–682. https://doi.org/10.1038/nmeth.2019 (2012).

Acknowledgements

The authors would like to express their sincere gratitude to François Hémard for his contributions to the acquisition, processing, and analysis of γ H2AX images, and to Axel Fontanier for his valuable help in brightfield image acquisition. Special thanks are extended to Elise Delage for her expert guidance on image analysis and fluorescence quantification. Finally, we warmly thank Florian Larramendy for his review of the manuscript. Funding sources include SupBiotech, CEA and NETRI company as well as the ANR funding CS_AGE. SupBiotech is part of the DIM C-BRAINS, funded by the Conseil Régional d'Ile-De-France. The authors declare that no other external funds, grants, or other support were received during the preparation of this manuscript.

Author contributions

All authors contributed to the study conception and design. Material preparation, data collection and analysis were performed by H.C., L.M., C.B., J.R. and P.-A.V. The first draft of the manuscript was written by H.C., J.R. and P.-A.V. and all authors commented on previous versions of the manuscript. All authors read and approved the final manuscript.

Declarations

Competing interests

H.C., C.B., B.G.C.M., J.R. and T.H. are employed by NETRI company, whose CEO and co-founder is T.H. The other authors declare no potential conflict of interest.

Additional information

Supplementary Information The online version contains supplementary material available at https://doi.org/1 0.1038/s41598-025-14425-x.

Correspondence and requests for materials should be addressed to H.C. or P.-A.V.

Reprints and permissions information is available at www.nature.com/reprints.

Publisher's note Springer Nature remains neutral with regard to jurisdictional claims in published maps and institutional affiliations.

Open Access This article is licensed under a Creative Commons Attribution 4.0 International License, which permits use, sharing, adaptation, distribution and reproduction in any medium or format, as long as you give appropriate credit to the original author(s) and the source, provide a link to the Creative Commons licence, and indicate if changes were made. The images or other third party material in this article are included in the article's Creative Commons licence, unless indicated otherwise in a credit line to the material. If material is not included in the article's Creative Commons licence and your intended use is not permitted by statutory regulation or exceeds the permitted use, you will need to obtain permission directly from the copyright holder. To view a copy of this licence, visit https://creativecommons.org/licenses/by/4.0/.

© The Author(s) 2025